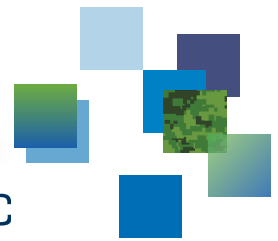




CAN UNCLASSIFIED



DRDC | RDDC
technologysciencetechnologie

The Kelvin Wake Infrared Radiance Model

Implementation into the Sea Surface Infrared Radiance Simulator

Vivian Issa

DRDC – Valcartier Research Centre

Zahir A. Daya

DRDC – Atlantic Research Centre

Defence Research and Development Canada

Scientific Report

DRDC-RDDC-2018-R246

February 2019

CAN UNCLASSIFIED

IMPORTANT INFORMATIVE STATEMENTS

This document was reviewed for Controlled Goods by DRDC using the Schedule to the *Defence Production Act*.

Disclaimer: Her Majesty the Queen in right of Canada, as represented by the Minister of National Defence ("Canada"), makes no representations or warranties, express or implied, of any kind whatsoever, and assumes no liability for the accuracy, reliability, completeness, currency or usefulness of any information, product, process or material included in this document. Nothing in this document should be interpreted as an endorsement for the specific use of any tool, technique or process examined in it. Any reliance on, or use of, any information, product, process or material included in this document is at the sole risk of the person so using it or relying on it. Canada does not assume any liability in respect of any damages or losses arising out of or in connection with the use of, or reliance on, any information, product, process or material included in this document.

Endorsement statement: This publication has been peer-reviewed and published by the Editorial Office of Defence Research and Development Canada, an agency of the Department of National Defence of Canada. Inquiries can be sent to: Publications.DRDC-RDDC@drdc-rddc.gc.ca.

© Her Majesty the Queen in Right of Canada, Department of National Defence, 2019

© Sa Majesté la Reine en droit du Canada, Ministère de la Défense nationale, 2019

Abstract

The well known ‘V’ shaped ship Kelvin wake consists of a pattern of sea surface waves with predictable elevation and orientation. In the middle wave infrared, the surface waves are simultaneously emitters and reflectors. The radiance pattern from the Kelvin wake can be exploited for strategic surveillance, smart tracking algorithms and for naval platform vulnerability assessment. We have modeled the middle wave infrared radiance of the Kelvin wake of a ship approximated by a point source of pressure on the surface of infinitely deep water. The elevation field of the Kelvin wake is normalized against measurements from a ship trial. This elevation input is then meshed into facets whose orientation are calculated numerically with a central finite difference scheme. Thereafter we have used the Sea Surface Radiance Simulator, a in-house Matlab code, to calculate the middle wave infrared radiance emitted and reflected by each facet toward an observer. The calculation takes into account the source-receiver geometry, the environmental radiometric sources, and the effects of propagation through the atmosphere. Since there are on the order of a million surface facets, we have clustered facets with the same slopes and relative receiver position. This clustering accelerates significantly the numerical calculation. We find that the mid wave infrared radiance of the Kelvin wake and its contrast with the sea surface background is highly dependent on the receiver position which determines which slopes in the wake are strongly reflecting and emitting in the direction of the receiver. Our Sea Surface Radiance Simulator, with the addition of the Kelvin wake modeling module, now has the capability to calculate the radiance of the three components of ship wakes (Kelvin, turbulent and white water) as well as that of the sea background. Experimental validation of the Kelvin wake midwave infrared radiance against a comprehensive measurement data set is currently being undertaken.

Résumé

Le « V » caractéristique du sillage de Kelvin créé par le passage d'un bateau consiste en un agencement d'ondes à la surface de la mer possédant une amplitude et une orientation prévisibles. Les ondes de surface sont simultanément émettrices et réfléchies dans l'infrarouge moyen. Le modèle de luminance énergétique produit par le sillage de Kelvin peut être exploité à des fins de surveillance stratégique, d'établissement d'algorithmes de poursuite intelligente et d'évaluation de la vulnérabilité de la plateforme navale. Nous avons modélisé la luminance énergétique du sillage de Kelvin d'un navire dans l'infrarouge moyen représentée approximativement par une source ponctuelle de pression à la surface d'eau de mer très profonde. Le champ des données d'amplitude du sillage de Kelvin est normalisé avec des mesures obtenues au cours d'essais réalisés avec un navire. Ces données d'amplitude ont ensuite été intégrées à des facettes dont l'orientation est calculée numériquement selon une méthode des différences finies. Par la suite, nous avons utilisé le programme de luminance énergétique à la surface de la mer, programme interne Matlab, pour calculer la luminance énergétique dans l'infrarouge moyen émise et réfléchi par chaque facette vers un observateur. Le calcul tient compte de la géométrie source récepteur, des sources radiométriques environnementales et des effets de la propagation dans l'atmosphère. Puisqu'il existe environ un million de facettes à la surface, nous les avons regroupées selon leur pente et leur position par rapport au récepteur. Ce regroupement accélère considérablement le calcul numérique. Nous avons découvert que la luminance énergétique dans l'infrarouge moyen du sillage de Kelvin et son contraste par rapport à la surface de la mer environnante dépend grandement de la position du récepteur. Celle-ci détermine quelles pentes du sillage reflètent fortement et émettent dans la direction du récepteur. Le programme de luminance énergétique à la surface de la mer, combiné au module de modélisation du sillage de Kelvin, a maintenant la capacité de calculer la luminance énergétique des trois composantes du sillage des navires (sillage de Kelvin, turbulences et bouillonnements) de même que la mer environnante. La validation expérimentale de la luminance énergétique dans l'infrarouge moyen du sillage de Kelvin par rapport à un ensemble exhaustif de données de mesure est toujours en cours.

Significance for defence and security

The Kelvin wake on the surface of the ocean caused by a naval vessel can be detected in the infrared. The variability in the detection of the Kelvin wake in the infrared is rather non-trivially related to a host of physical and geometrical parameters. The mathematical model developed here for the Kelvin wake in the infrared and incorporated in the Sea Surface Radiance Simulator facilitates the computation of the infrared contrast of the Kelvin wake and thereby its detection for the large number of physical and geometrical parameters. It thus provides useful guidance of when, in what conditions, and from where the Kelvin wake of a naval vessel is most detectable. These results constitute part of the input to a ship signature management tool aimed at providing operator guidance of a ship's degree of stealth.

Importance pour la défense et la sécurité

Le sillage Kelvin d'un navire peut être détecté dans l'infrarouge. La variabilité de détectabilité plutôt non triviale du sillage Kelvin est reliée à un ensemble des paramètres physiques et géométriques. Le modèle mathématique du sillage Kelvin dans l'infrarouge que nous avons développé dans ce travail et incorporé dans le Sea Surface Simulator facilite le calcul numérique du contraste infrarouge du sillage et ainsi sa détection pour un grand nombre des paramètres physiques et géométriques. Il fournit des indications utiles sur le moment, les conditions et les positions d'observateur où le navire est le plus détectable. Ces résultats peuvent être des entrées pour un logiciel de gestionnaire de signature dont le but est de fournir des recommandations aux opérateurs de leur degré de furtivité.

Table of contents

| | |
|-----------------------------------------------------------------------------------------------------|-----|
| Abstract | i |
| Résumé | ii |
| Significance for defence and security | ii |
| Importance pour la défense et la sécurité | iii |
| Table of contents | iv |
| List of figures | v |
| 1 Introduction | 1 |
| 1.1 The Kelvin Wake | 2 |
| 1.2 The Sea Surface Radiance Simulator | 4 |
| 2 Modeling the Infrared Radiance of the Kelvin Wake | 5 |
| 2.1 Point source gravity wave water elevation calculation and implementation into SSRS | 8 |
| 2.2 Kelvin Wake sea surface facets orientation | 11 |
| 2.3 Infrared Radiance of the Ship Kelvin wake | 12 |
| 3 Discussion and results | 14 |
| 4 Conclusion | 18 |
| References | 19 |
| Annex A: Note on the point of source Kelvin wake singularities | 20 |

List of figures

| | | |
|------------|-----------------------------------------------------------------------------------------------------------------------------------------------------------------------------------------------------------------------------------------------------------------------------------------------------------------------------------------------|----|
| Figure 1: | The Kelvin wake pattern captured by a FLIR SC6000 MWIR camera at the CFMETR range in Nanoose Bay in 2015. | 1 |
| Figure 2: | At each angular position there is a transverse (blue) and divergent (red) wave. | 3 |
| Figure 3: | Sea Surface Radiance Simulator: basic flow chart. | 4 |
| Figure 4: | Sea Surface Radiance Simulator Flow Chart with modules for the background and wake components. | 6 |
| Figure 5: | The SSRS flowchart showing the Kelvin wake modules. | 7 |
| Figure 6: | The maximum wave amplitude for wave cuts at 100, 500 and 1000 meter for Quest at three different speed (red, blue and green for respectively 9, 12, 15 kts) given by Hally [10, 11] (dotted line), for a point of source with Whitham original equation (Equation 1) (dashed line) and by SSRS with the Equation 5 (continuous line). | 9 |
| Figure 7: | Transverse, Divergent and total Kelvin wave of a disturbance point traveling at a constant speed in a deep water of 15 knots (Left) and 12 knots (right). The speed of the point pressure source is manifested in the wavelength of the KW pattern. | 10 |
| Figure 8: | X component of the sea surface meshes orientation (Z_x) (left) and the Y component of the sea surface meshes orientation (Z_y). | 12 |
| Figure 9: | Histogram of relative receiver zenith angle (left) and azimuth angle for the Kelvin wake up to 300 m of radial distance for a receiver at $(x, y, z) = (0, -800, 30)$ meter from the ship. | 13 |
| Figure 10: | Histogram of the Z_x (left) and Z_y (right) facets slopes for the Kelvin wake up to 300 m of radial distance for a receiver at $(x, y, z) = (0, -800, 30)$ meter from the ship. | 13 |
| Figure 11: | Radiance of the Kelvin wake toward a receiver for scenario 1 (top) scenario 2 (middle) scenario 3 (bottom). | 15 |
| Figure 12: | The Kelvin wake asymmetrical radiance captured by a FLIR SC6000 MWIR camera at the CFMETR range in Nanoose Bay in 2015. | 16 |
| Figure 13: | % of the contrast of the radiance between scenario 1 and 2 (top) and the contrast of the radiance between scenario 3 and 2 (bottom). | 17 |

Figure A.1: The term $\cos^{5/2}\psi$ in the divergent wave (left) and in the transverse
wave (right). 20

1 Introduction

Any object on the sea surface with a relative speed to the water perturbs the interface resulting in gravity waves known as the Kelvin wake (KW). In the middle wave infrared (MWIR), the KW appears as a pattern of sea surface facets with predictable orientations reflecting the sky, sun or other radiometric sources while at the same time emitting their own radiance. These KW facets with well defined orientations have a contrast with the background sea surface radiance. The KW facets have regular spatial and temporal features that are different from the background clutter.

The MWIR KW contrast, while strongly dependent on relative position of the wake-receiver geometry, is often rich in information about the KW source such as its position, size, speed and heading. In a defense context, either for strategic surveillance, smart tracking algorithms or for naval platform vulnerability assessment, a deep understanding and modeling capability of the KW infrared radiance is crucial. In Figure 1 we show an image of a ship KW pattern in the MWIR.

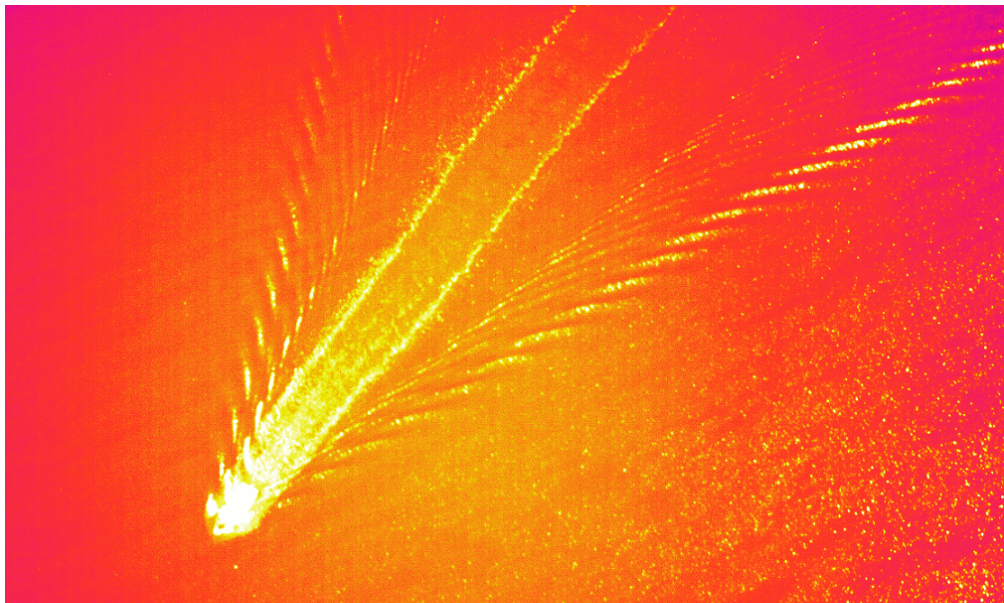


Figure 1: The Kelvin wake pattern captured by a FLIR SC6000 MWIR camera at the CFMETR range in Nanoose Bay in 2015.

In modelling the KW in the MWIR it is necessary to fully model the sea surface in the infrared [1]. We have previously introduced our Sea Surface Radiance Simulator (SSRS) with which we have successfully modeled the sea surface background and the turbulent wake trailing a ship [1, 2, 3, 4]. The SSRS is an in-house Matlab code that calculates the total infrared radiance (emitted and reflected) for any sea surface with a known probability density function (pdf) of sea surface slopes. The code requires a large number of input variables such as the sea surface and air temperatures, the relative humidity, the atmospheric

pressure, the wind speed, the geographical location and time of the diurn, the ship position and receiver characteristics to account for the target-observer geometry, the propagation through the atmosphere and spectral response of the receiver.

In the following two subsections we introduce our model of the Kelvin wake and the functional capability of the SSRS. In Section 2 we discuss our modeling of the KW infrared radiance and in Section 3 we present our results and discuss the dependence of the KW MWIR radiance on temperature of the sea surface and on the relative position of the receiver.

1.1 The Kelvin Wake

Since Sir William Thompson first provided the mathematical description of the ship wave pattern in 1879, the Kelvin wake has been extensively published in the scientific literature. Its mathematical description is in constant evolution. Reed *et. al.* [5] presented an elegant description of the KW pattern and a brief history on the evolution of the mathematics of the wave problem. He also provided a solution and mathematical development of the complex boundary of the KW.

Whitham [6] presented in his book a detailed formulation of the problem and solution. He showed that the surface height perturbation at an angular position (r, ξ) from a ship moving at a speed u can be approximated to the solution of the two dimensional problem of gravity waves, produced by a point source disturbance, given by

$$\eta(r, \xi) \approx -\sqrt{\frac{2g}{\pi r}} \frac{p}{u^3 \cos^3 \psi} \frac{(1 + 4 \tan^2 \psi)^{1/4}}{|1 - \tan^2 \psi|^{1/2}} \sin \left\{ rk \cos(\psi + \xi) + \frac{\pi}{4} \text{sgn} \left(s''(\psi) \right) \right\}, \quad (1)$$

where g is the gravitational acceleration, p is the pressure function created by the ship on the sea surface, $k = \frac{g}{u^2 \cos^2 \psi}$ is the wave vector oriented at ψ from the ship heading. The wave propagation angle ψ and the angular position ξ are related by $\tan(\psi + \xi) = 2 \tan(\psi)$. The sign function in Equation 1 is given by Equation 2.

$$\text{sgn} \left[s''(\psi) \right] = \text{sgn} \left[k \cos(\psi + \xi) \left[\frac{2}{\cos^2 \psi} - (1 + 4 \tan^2 \psi) \right] \right]. \quad (2)$$

The relation between the wave heading ψ and the angular position ξ is satisfied by two headings for each angular position,

$$\tan(\psi) = \frac{1 \pm \sqrt{1 - 8 \tan^2 \xi}}{4 \tan \xi}, \quad (3)$$

one is for the divergent wave and the other for the transverse waves. In Figure 2 we have plotted the transverse and divergent wave headings for each angular position.

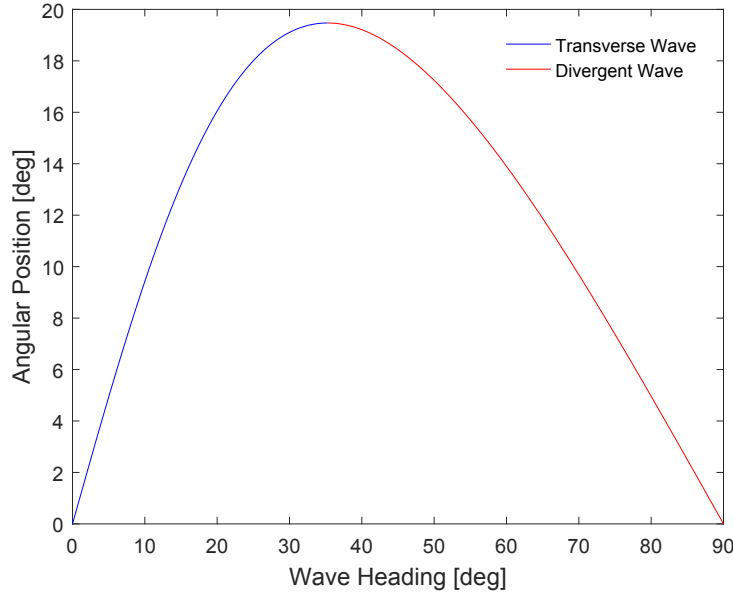


Figure 2: At each angular position there is a transverse (blue) and divergent (red) wave.

The angular position of wave crests ξ has a maximum at $\xi_{max} = \text{atan}(\pm \frac{1}{2\sqrt{2}}) = 19.5^\circ$ where $\tan(\psi) = \frac{1}{\sqrt{2}}$. This result is independent of the ship speed; it derives from the fact that the ratio of the group velocity to the phase velocity is equal to $1/2$ for deep water waves. That the ‘V’ shape of the KW has limiting arms at an angle of 19.5° to the central downstream line is a consequence of this fact.

Whitham’s approximation of the KW (Equation 1) is valid for a ship traveling at constant velocity in deep water and is taken ad hoc as a point source of pressure. In this approximation, the surface tension and viscosity are neglected and the free surface boundary conditions (velocity and pressure at the free surface) are linearized.

This approximation fails at two singularities: at the edge of ‘V’ wedge where $\xi \rightarrow \xi_{max}$ and at the central downstream line where $\xi \rightarrow 0$. The first singularity is at the arms of the wedge where the Kelvin wake is confined. At this maximum angular position of the pattern, the divergent and transverse crests wave meet at a cusp. The second singularity is a consequence of assuming that the ship is modeled by a point pressure disturbance. Ursell [7] has presented an elegant detailed study of these singular regions. This singularity does not affect our modeling since the central line of the ship downstream wake is where the turbulent wake occurs and its adequately modeled in the SSRS [2, 3, 4]. Furthermore, in the foregoing approximation, the ship which is considered as a point source means that the impact of the ship hull shape on the KW is not captured in our model. Our model of the

KW pattern is confined to within the two singularities and does not address the bow wave that is specific to ship hulls.

1.2 The Sea Surface Radiance Simulator

We have developed a Sea Surface Radiance Simulator (SSRS) over the last few years to accurately model the sea surface radiance in the infrared for a range of sea surface condition including multiple ship wake phenomena[2, 3, 4]. Our SSRS code is implemented in Matlab and is designed to accommodate the effects of the Kelvin, white water and turbulent wakes superimposed on a stochastic sea surface background taking into account the enviromental radiometric sources and the effects of propagation through the atmosphere. In Figure 3 we show a basic flow chart of the SSRS.

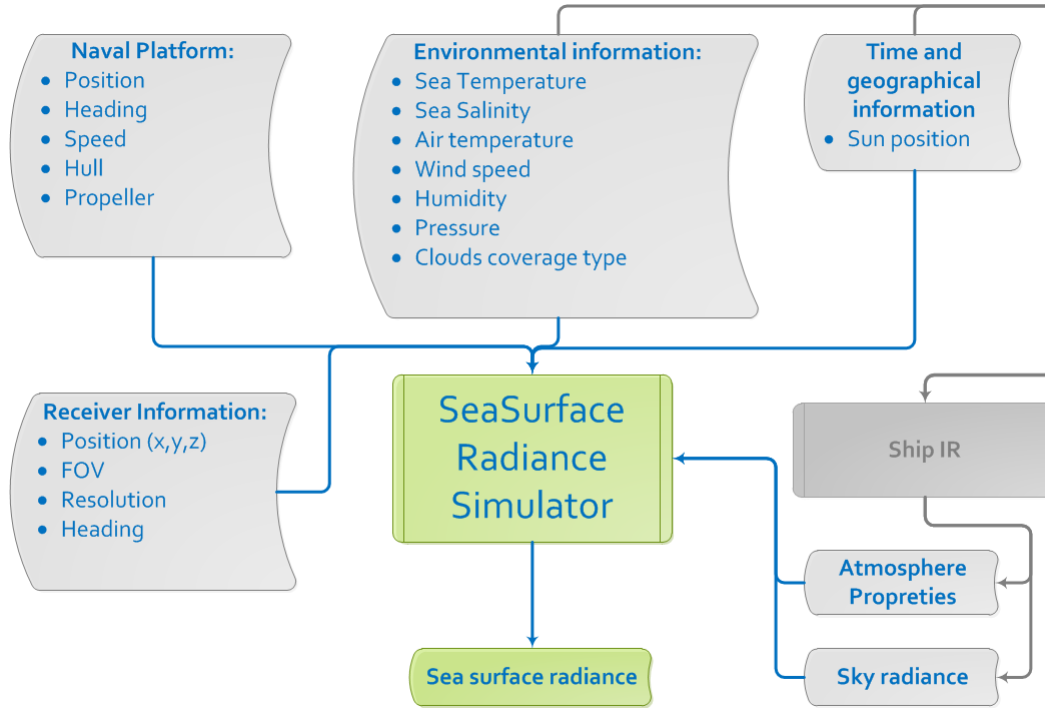


Figure 3: Sea Surface Radiance Simulator: basic flow chart.

In our modeling of the sea surface radiance, we consider the sea surface as an ensemble of facets where each facet is defined by its slopes (z_x, z_y). The amount of radiance that each facet contributes to the total radiance received by a camera pixel is related to the slope probability density function and the receiver position. Our modeling of the sea surface infrared radiance background [2, 3] includes the contribution of each facet toward the receiver based on the Cox and Munk [8] pdf. In modeling the turbulent wake [4] and the white water wake [9], we have built our own facet slope pdf based on the phenomenology of the turbulence and the bubble distributions in ship wakes.

Once the overall pdf of the sea surface is determined *i.e.* the pdf of slopes in the background and in each of the wake zones, the contribution from each facet with orientation (z_x, z_y) to the total radiance received by a camera pixel is calculated in Equation 4.

We have shown in [4] that total spectral radiance $L(\lambda, T, \theta_r, \phi_r)$ outgoing from an area seen by one pixel is given by

$$L(\lambda, T, \theta_r, \phi_r) = \underbrace{\int \int_{\omega \leq \frac{\pi}{2}} \frac{dA_r(\theta_r, \phi_r, z_x, z_y)}{A_r(\theta_r, \phi_r)} L(\lambda, T, \theta_r, \phi_r, z_x, z_y) dz_x dz_y}_{\omega \leq \frac{\pi}{2}} \quad (4)$$

where the fractional area toward the receiver $\frac{dA_r(\theta_r, \phi_r, z_x, z_y)}{A_r(\theta_r, \phi_r)}$ corresponds to the contribution of each facet to the radiance received by the detector. A_r is the total area projected toward the receiver, and $dA_r(\theta_r, \phi_r, z_x, z_y)$ is the projection of the facet with slopes z_x, z_y toward the receiver.

In Figure 4 we show a more detailed SSRS flowchart that includes the modules for the background IR radiance and for each of the three components of ship wakes: the Kelvin wake, the turbulent wake and the white water wake.

2 Modeling the Infrared Radiance of the Kelvin Wake

In Figure 5 we show the flowchart of how the KW infrared radiance is modeled in the SSRS. In this diagram cylinders represents input variables to the different modules. Grey boxes represent the already existing modules in SSRS. Orange boxes represent the new modules implemented in the SSRS to calculate the KW radiance. The dashed red box represents the standard SSRS flowchart shown in Figure 4 with the updated modules in the green boxes.

The first module added to the SSRS addresses mapping of the KW area on the sea surface. This module creates nodes for meshing the sea surface into facets from the central line downstream the ship until the KW wedge at $\text{atan} \frac{1}{2\sqrt{2}}$. Since capillary waves are neglected in our KW model, we used a maximum radial resolution of 2 cm in our simulation. In general, in the SSRS, angular and radial resolutions are controlled by the user.

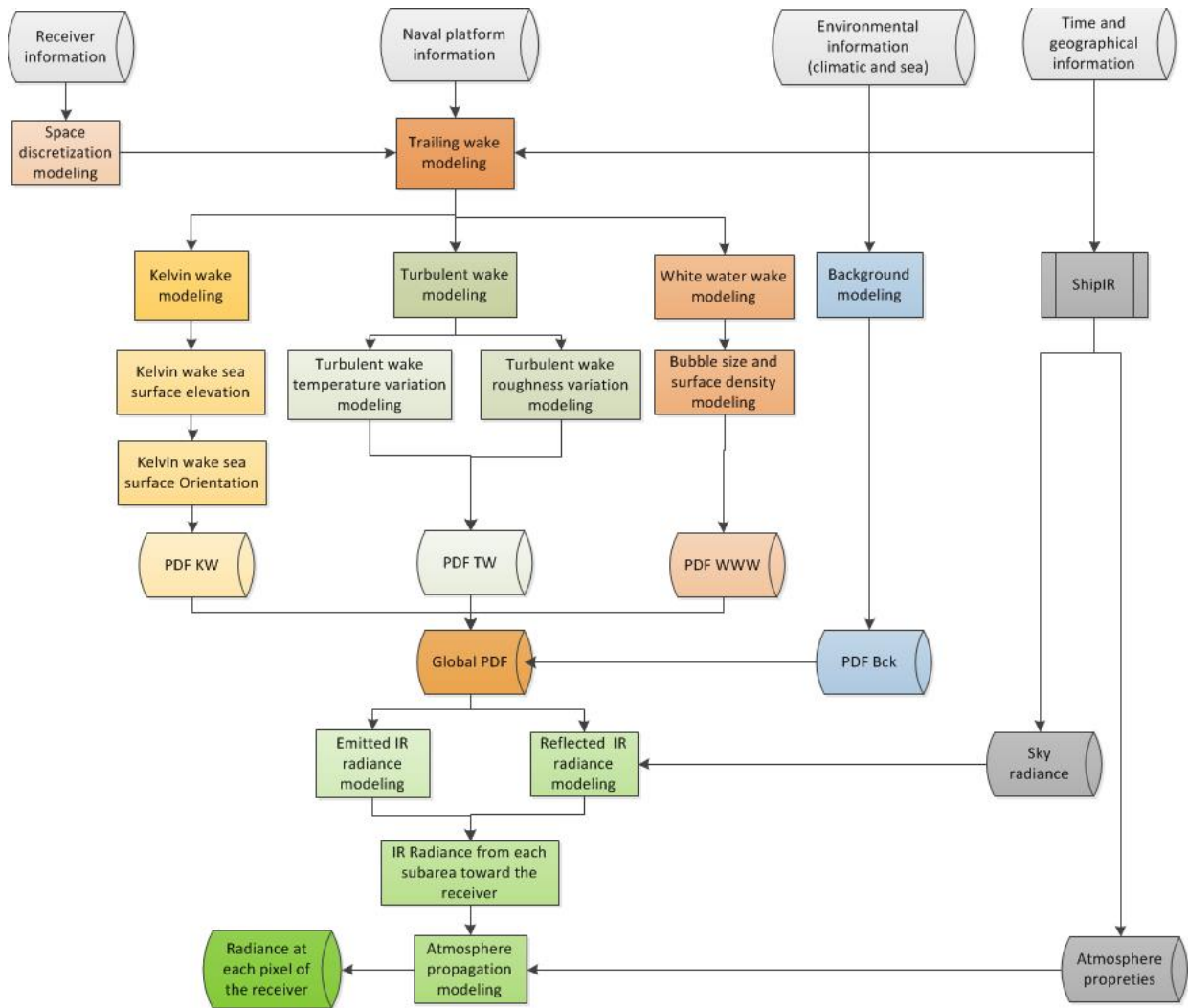


Figure 4: Sea Surface Radiance Simulator Flow Chart with modules for the background and wake components.

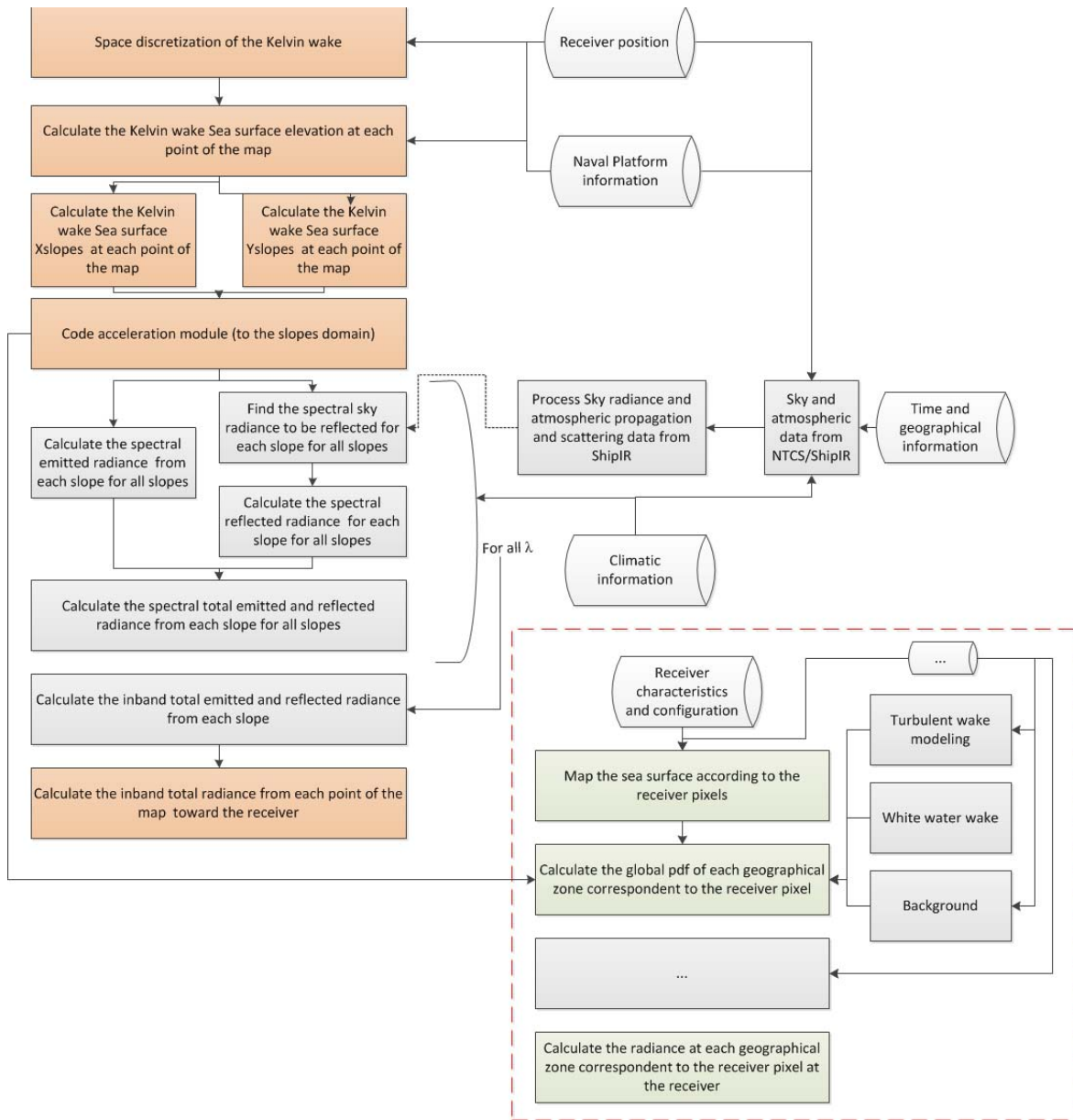


Figure 5: The SSRS flowchart showing the Kelvin wake modules.

2.1 Point source gravity wave water elevation calculation and implementation into SSRS

Since our aim in this work is to calculate the IR radiance of the KW rather than to accurately calculate the KW sea surface elevation itself, we approximate the elevation of a ship KW with that of a point source of pressure traveling at constant speed on the surface of an infinitely deep sea. Even though this approximation does not capture the ship specific wake effects, it is a good starting point for a sea surface elevation input to SSRS. We use Whitham approximation given in Equation 1 multiplied by the term $\cos^{5/2}\psi$ to eliminate the singularity within the central area of the wake. We show in Annex A a brief analysis behind our choice for the multiplicative term added to the equation. Hence, the Equation 1 becomes

$$\eta(r, \xi) \approx -\sqrt{\frac{2g}{\pi r}} \frac{p}{u^3 \cos^{1/2}\psi} \frac{(1 + 4\tan^2\psi)^{1/4}}{|1 - \tan^2\psi|^{1/2}} \sin \left\{ rk\cos(\psi + \xi) + \frac{\pi}{4} \text{sgn} \left(s''(\psi) \right) \right\}, \quad (5)$$

In order to compare the SSRS KW elevations with measurements, we normalize the calculated elevation with the results of CFAV Quest given by Hally [10, 11]. The normalization was achieved by multiplying the amplitude, at a given speed, by the ratio of the maximum amplitude given by Hally's results to the maximum amplitude at one of the three given range.

In Figure 6 we compare the Hally measurements of the maximum wave amplitudes versus those from a point source modeled by Equations 1 and 5. We normalize the point source amplitudes against the Hally measurements at the 100m offset for each speed ¹. After normalization the wave amplitudes from Equation 5 are within the error bars of the Hally measurements for all speeds and offsets that were measured. On the other hand the singularity in Equation 1 is detrimental to estimating the wave amplitude field in the KW.

In Figure 7 we show respectively the results of the transverse and divergent wave components of the KW as well as the total elevation of the sea surface in the KW simulated with SSRS for a point pressure source cruising at 15 and 12 knots respectively. The magnitude of the point pressure source is arbitrary.

¹ We have to note that the normalization was done for each ship speed (u) since Hally results are dependent on u^2 while the point of source solution is dependent on the $u^{-1/3}$.

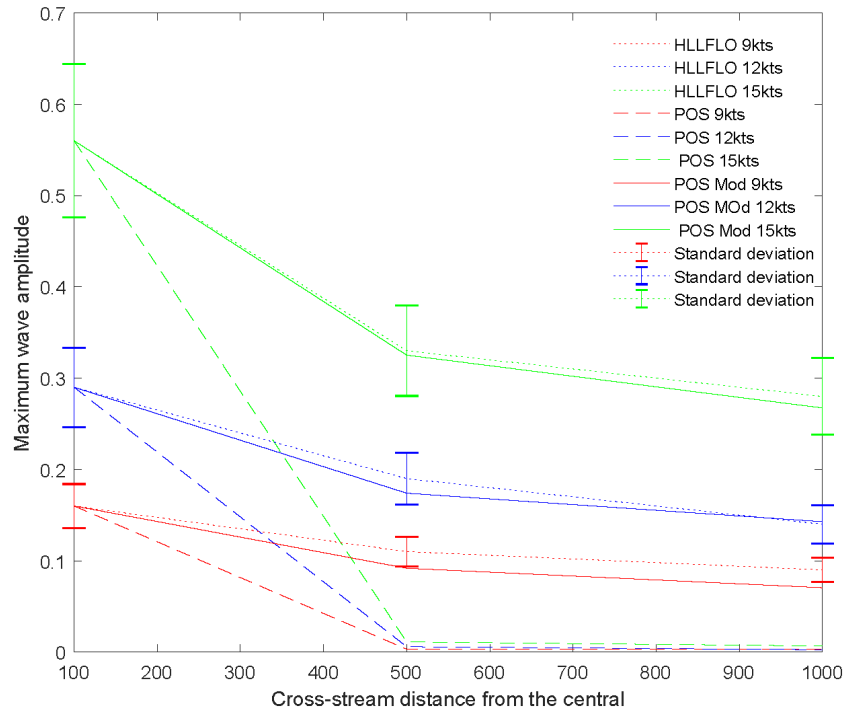


Figure 6: The maximum wave amplitude for wave cuts at 100, 500 and 1000 meter for Quest at three different speed (red, blue and green for respectively 9, 12, 15 kts) given by Hally [10, 11] (dotted line), for a point of source with Whitham original equation (Equation 1) (dashed line) and by SSRS with the Equation 5 (continuous line).

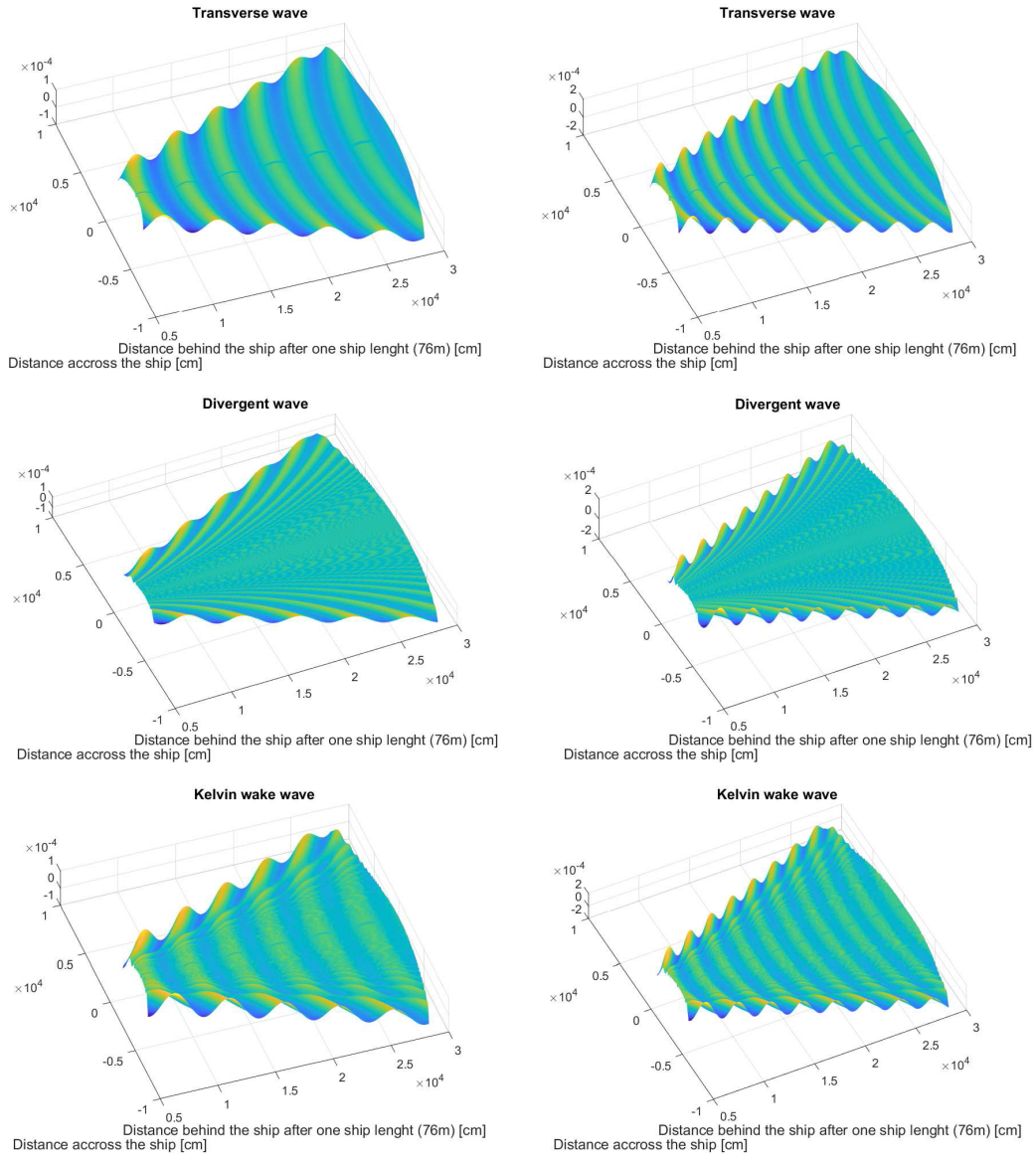


Figure 7: Transverse, Divergent and total Kelvin wave of a disturbance point traveling at a constant speed in a deep water of 15 knots (Left) and 12 knots (right). The speed of the point pressure source is manifested in the wavelength of the KW pattern.

2.2 Kelvin Wake sea surface facets orientation

Given the sea surface elevation, SSRS calculates the orientation of sea surface facets and then calculates the radiance emitted and reflected by them. The mesh orientations Z_x and Z_y are calculated in the second module added to the SSRS. The gradient of the sea surface in the KW is

$$(Z_x, Z_y) = \nabla\eta(r, \xi). \quad (6)$$

After conversion from cylindrical to cartesian coordinates, the gradient expression becomes

$$\nabla\eta(r, \xi) = \left[\frac{\partial\eta}{\partial r} \cos\xi - \frac{1}{r} \frac{\partial\eta}{\partial \xi} \sin\xi \right] \hat{x} + \left[\frac{\partial\eta}{\partial r} \sin\xi + \frac{1}{r} \frac{\partial\eta}{\partial \xi} \cos\xi \right] \hat{y} + \frac{\partial\eta}{\partial z} \hat{z}, \quad (7)$$

and hence the meshes slopes orientations Z_x and Z_y can be calculated with

$$\begin{aligned} Z_x &= \left[\frac{\partial\eta}{\partial r} \cos\xi - \frac{1}{r} \frac{\partial\eta}{\partial \xi} \sin\xi \right] \\ Z_y &= \left[\frac{\partial\eta}{\partial r} \sin\xi + \frac{1}{r} \frac{\partial\eta}{\partial \xi} \cos\xi \right]. \end{aligned} \quad (8)$$

$\frac{\partial\eta}{\partial r}$ and $\frac{\partial\eta}{\partial \xi}$ are calculated numerically with a central finite difference scheme

$$\frac{\partial\eta}{\partial r} \Big|_{r=r_i} = \frac{\eta(r_{i+1}) - \eta(r_{i-1}))}{r_{i+1} - r_{i-1}}, \quad (9)$$

and

$$\frac{\partial\eta}{\partial \xi} \Big|_{\xi=\xi_i} = \frac{\eta(\xi_{i+1}) - \eta(\xi_{i-1}))}{\xi_{i+1} - \xi_{i-1}}. \quad (10)$$

In Figure 8 we show the slopes for the X and Y components of the sea surface mesh orientations (Z_x) (left) and (Z_y) (right). These results were generated for a radial resolution of 10 cm and angular resolution of 0.0044 rad resulting in more than 3 million facets in each mesh.

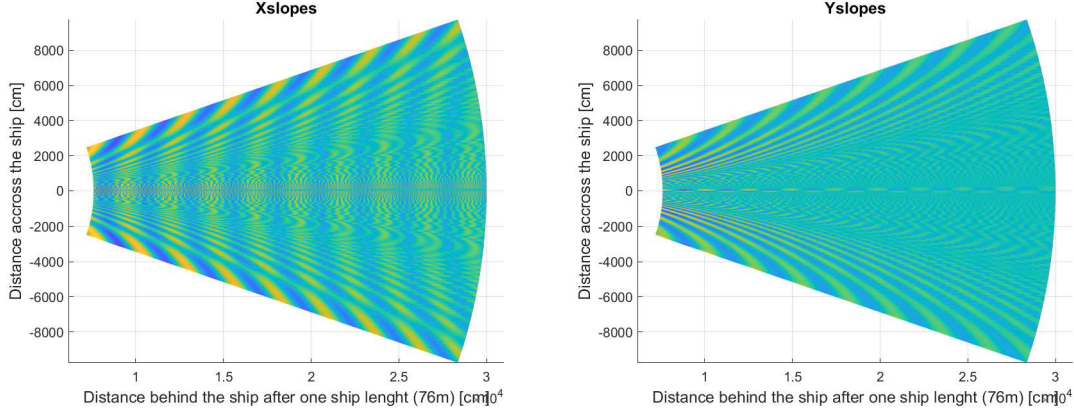


Figure 8: X component of the sea surface meshes orientation (Z_x) (left) and the Y component of the sea surface meshes orientation (Z_y).

2.3 Infrared Radiance of the Ship Kelvin wake

When the sea surface facet orientation is known, the radiance toward a receiver becomes the addition of the emitted radiance (L_e) and the reflected radiance (L_r):

$$\begin{aligned}
 L(\lambda, T, \theta_r, \phi_r,) &= L_e(\lambda, T, \theta_r, \phi_r, z_x, z_y) + L_r(\lambda, \theta_r, \phi_r, z_x, z_y) \\
 &= [1 - \rho(\omega, \lambda)] \times P(T, \lambda) \\
 &+ \rho(\omega) \times L_s(\lambda, \theta_s, \phi_s),
 \end{aligned} \tag{11}$$

where $\rho(\omega, \lambda)$ is the spectral reflectivity of the sea surface in the direction of the receiver. $L_s(\lambda, \theta_s, \phi_s)$ is the sky radiance arriving at the facet from the direction (θ_s, ϕ_s) where θ_s and ϕ_s are the coordinates of the part of sky reflected on the facet and they are dependent on the receiver position and mesh orientation $(\theta_r, \phi_r, z_x, z_y)$.

In order to accelerate the code, instead of calculating the emitted, reflected and total spectral and in-band radiance for each of these facets, we identify among them those which have the same relative position with respect to the receiver and the same facet slopes. These facets contribute equally and so need only be computed once.

Lets take the case for a receiver at $(x, y, z) = (0, -800, 30)$ meters from the ship where (x, y, z) are the coordinates axes that correspond respectively to the downstream, crosstream and vertical directions. In Figures 9 and 10 we show the histograms of relative receiver zenith angle, azimuthal angle and the X and Y components of the sea surface facet orientations. Hence, to prevent redundant calculation, the data is restructured and facets with the same orientation and relative receiver position are associated to a unique classification code.

All the facets with the same classification code will be associated to the same radiance. And hence, the radiance calculation is called only once for each combination of relative receiver position and facet orientation. The radiance for hidden facets is not calculated as they do not directly radiate toward the receiver. By selectively grouping the contributions in this way, the code acceleration module speeds up the computation time from several day to minutes.

For each facet of the KW where the radiance calculation module is executed, the SSRS calculates the emitted and reflected radiance using the same approach described in our previous papers [2, 3, 4] with Equation 11.

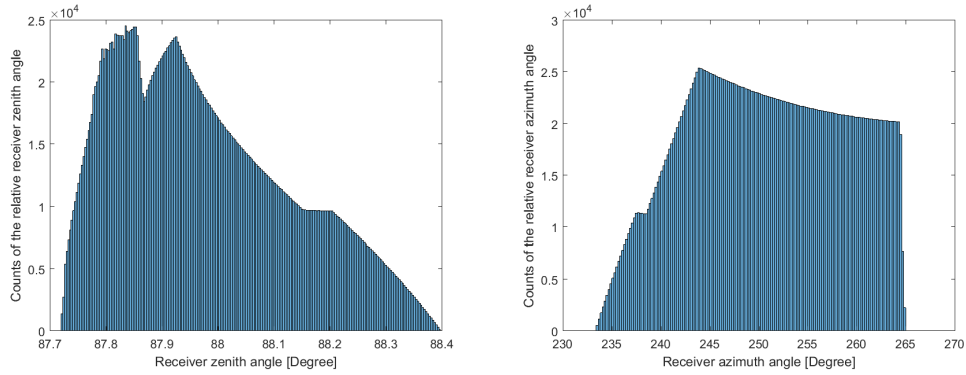


Figure 9: Histogram of relative receiver zenith angle (left) and azimuth angle for the Kelvin wake up to 300 m of radial distance for a receiver at $(x, y, z) = (0, -800, 30)$ meter from the ship.

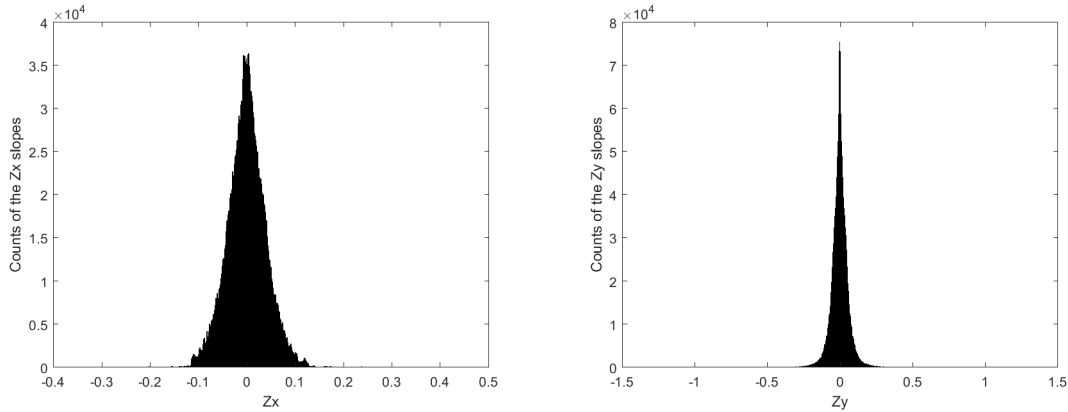


Figure 10: Histogram of the Z_x (left) and Z_y (right) facets slopes for the Kelvin wake up to 300 m of radial distance for a receiver at $(x, y, z) = (0, -800, 30)$ meter from the ship.

3 Discussion and results

We have modeled the elevation, the orientation and the MWIR radiance of the sea surface within the KW. Our modeling is implemented in the SSRS to calculate the infrared radiance toward a specific receiver position for the KW from the research vessel Quest.

In Figure 11, we show the radiance of the Kelvin wake for the Quest for scenarios 1, 2 and 3 described in Table 1. In the first two scenarios, we have used the same atmosphere, sky conditions and receiver position but different sea surface temperatures. The third scenario is the same to the second scenario except for the receiver position. Facets without radiance values within the Kelvin wake are the hidden facets toward the receiver. While the sea surface elevation is symmetric with respect to the central line, the infrared radiance of the KW is asymmetrical. This is expected since symmetrical facets, while they have the same elevation, they do not have neither the same orientation nor the same relative receiver position. In Figure 12 we show an image of an asymmetrical infrared radiance.

Table 1: Background parameters for scenario 1 and the different parameters in scenarios 2 and 3.

| | Scenario 1 | Scenario 2 | Scenario 3 |
|---------------------------------|----------------------|------------|---------------|
| Sky Type | Clear without clouds | | |
| Wind Direction | North (90°) | | |
| Wind Speed | 1 m/s | | |
| Relative Humidity | 76% | | |
| Ambient Temperature | 15.3°C | | |
| Sea Temperature | 12°C | 4°C | 4°C |
| Location | Long 63.1 Lat 44.2 | | |
| Time | 2000 GTM | | |
| Sun position | Az 204.73 Zen 74.85 | | |
| Receiver position | (0,-800,30) | | (951,323,209) |
| With respect to the ship | | | |
| Zenith;Azimuth | (87.8, -90) | | (78.24, 18.7) |
| With respect to the ship | | | |

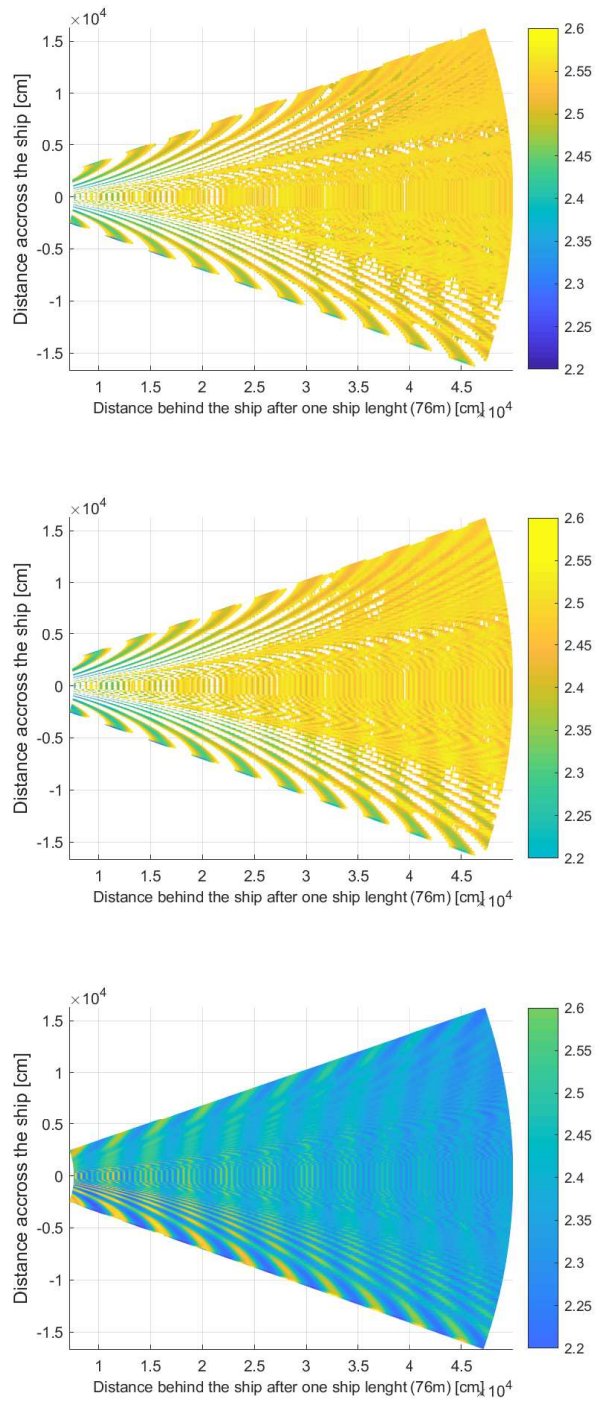


Figure 11: Radiance of the Kelvin wake toward a receiver for scenario 1 (top) scenario 2 (middle) scenario 3 (bottom).

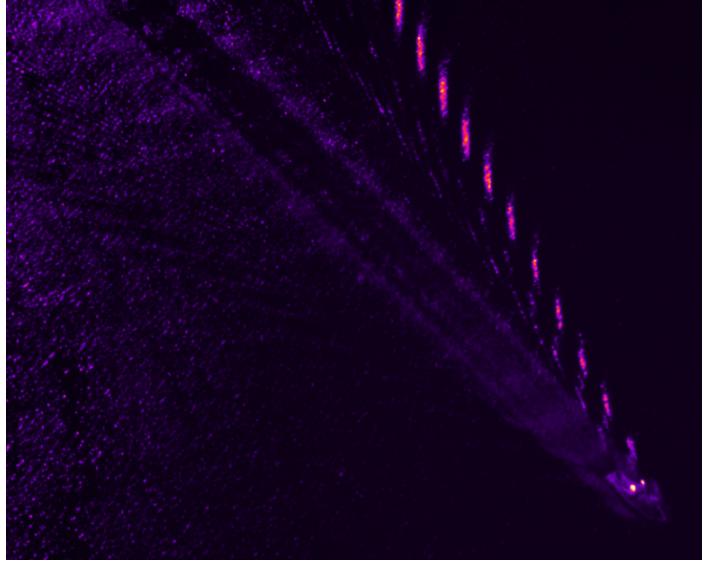


Figure 12: The Kelvin wake asymmetrical radiance captured by a FLIR SC6000 MWIR camera at the CFMETR range in Nanoose Bay in 2015.

The variation in the sea surface temperature between scenario 1 and 2 has a greater impact on the radiance of the KW facets with increasing omega, the angle between the normal to the facet and the receiver relative position to the facet. These facets which have a smaller angle of incidence for a low zenith receiver and hence higher emissivity as shown in Figure [10] of [4]. In the top part of the Figure 13, we show the percentage of contrast between the radiance of the KW in scenario 1 and 2. Since the sea temperature decreases in scenario 2 compared to scenario 1, the emitted radiance decreases and hence the total radiance contrast is positive. Note that we define the contrast by

$$L_{12} = \frac{L_1 - L_2}{L_2} * 100. \quad (12)$$

The variation in the receiver position between scenario 2 and 3 highlights the receiver position significant impact on the radiance of the KW. For the same facets orientation of the sea surface, by varying the receiver position, the incidence angle of each facets varies and hence so do the emissivity and reflectivity. In the bottom part of the Figure 13, we show the percentage of contrast between the radiance of the KW in scenario 3 and 2 which they do have same temperature but different receiver position, the contrast L_{32} vary from -10% up to 40% at different position in the wake . Note that there are less hidden facets in scenario 3 than in scenario 1 and 2 since the receiver zenith angle is lower.

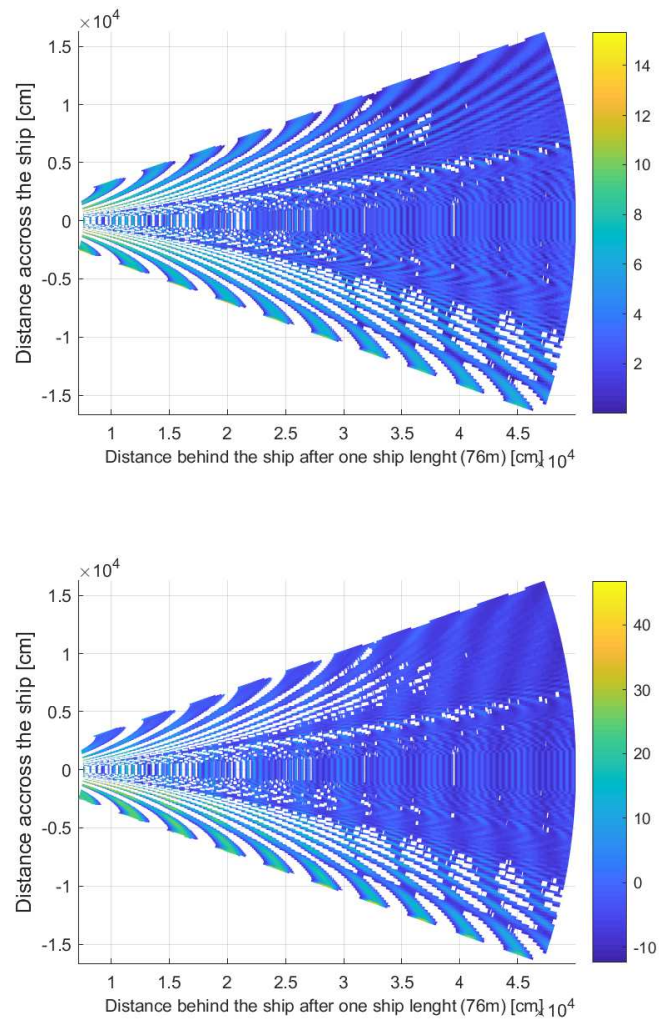


Figure 13: % of the contrast of the radiance between scenario 1 and 2 (top) and the contrast of the radiance between scenario 3 and 2 (bottom).

The approximation of the ship by point of source traveling through the water and the use of the measurements of the KW amplitude from a ship trial to normalize the sea surface height in our first module, offers a simple and low computational cost pattern of the Kelvin wake. Although, it does not contain the wave system details that are specific to the hull shape and it is not calculated in our case for the singularities regions and near the ship, the model remains valid in the majority of the KW. An experimental study for the evaluation of the accuracy of our modeling should be done followed by a study on the impact of the hull geometry on the Kelvin wake MWIR radiance.

Although, the contrast created by the KW has its own regularities that are different from the clutter of the background, including a clutter modeling of the sea surface background within the SSRS will further our understanding of the KW contrast in sea surface backgrounds of variable clutter.

4 Conclusion

We have modeled the elevation and orientation of the sea surface within the KW and taking into account the various radiometric sources and the relative position of the observer, we have calculated the MWIR radiance leaving the KW. Our modeling is implemented in the SSRS where we have applied the calculation for the KW MWIR radiance for the KW of CFAV Quest moving at a known speed and heading in an environment that is described accurately with respect to atmospheric parameters and solar position. Our results show the high dependence of the infrared radiance of the KW and its contrast with the background on the receiver position.

Improving the sky radiance model input into SSRS with higher resolution and including the sun radiance for a more realistic solar disc source than the point source that is currently used will allow us to study the glint on the Kelvin wake. Furthermore including a clutter model of the sea surface background within the SSRS will facilitate a more accurate contrast of the KW with the background.

A fuller comparison with experimental data beyond the limited comparison undertaken here should be completed in the fullness of time. In particular it is important to study the variation of the measured elevation data over a broad range of the KW systematically for various ship speeds and in several differently cluttered sea backgrounds. Additionally the impact of the hull geometry on the KW elevations especially at or near the theoretical singularities can substantially improve the KW models that can be used in SSRS to compute the MWIR radiance. For such study, measurements of the Kelvin wake of a ship should be taken and the sea surface elevation of the Kelvin wake of a specific hull can be calculated with one of the existing software such POTFLOW and CHERIE. The SSRS can thereafter use the elevation fields from these software to calculate the sea surface orientation and the spectral and inband MWIR radiance of the Kelvin wake. A study on the different existing software and their performance is required and should be followed by study the impact of the different hull specifications on the MWIR radiance of the ship Kelvin wake.

References

- [1] Daya, Z. A. and Hutt, D. L. (2010), Rudiments of Ship Wakes in the Infrared, *DRDC Atlantic TN 2010-168*.
- [2] Issa, V. and Daya, Z. A. (2010), Sea Surface Infrared Radiance Simulator Part 1: Roughness and Temperature models of the Sea Surface Radiance, DRDC Atlantic TM 2010-280, Defence R&D Canada - Atlantic.
- [3] Issa, V. and Daya, Z. A. (2010), Sea Surface Infrared Radiance Simulator Part 2: Sky Radiance and Trailing wake Integration models of the Sea Surface Radiance, DRDC Atlantic TM 2011-325, Defence R&D Canada - Atlantic.
- [4] Issa, V. and Daya, Z. (2014), Modeling the turbulent trailing ship wake in the infrared, *Applied Optics*, 53, 4282–4296.
- [5] Reed, A. M. and Milgram, J. H. (2002), Ship wakes and their radar images, *Annual Review of Fluid Mechanics*, 34, 469–502.
- [6] Whitham, G. (1973), *Linear And Non Linear Waves*, John Wiley and Sons.
- [7] Ursell, F. (1959), On Kelvin’s ship-wave pattern, Department of Applied Mathematics and theoretical physics.
- [8] Cox, C. and Munk., W. (1954), Measurement of the Roughness of the Sea Surface from Photographs of the sun Glitter, *Journal of the Optical Society of America*, 44, 838.
- [9] Issa, V. and Daya, Z. (in press), Modeling the infrared radiance of the white water wake, *submitted to applied optics*.
- [10] Hally, D. (1997), Wave amplitude in the far wake of CF ships, DREA TM 1997-220, Defence Research Establishment Atlantic.
- [11] Hally, D. (1993), Dispersion analysis of an unsteady free surface panel method, DREA TM 1993-211, Defence Research Establishment Atlantic.

Annex A Note on the point of source Kelvin wake singularities

At the central line of the KW pattern, when $\xi = 0$, ψ becomes equal to 0 in the transverse wave and to $\pi/2$ in the divergent wave (Figure 2). With this last case, the term $\frac{(1+4\tan^2\psi)^{1/4}}{\cos^3\psi|1-\tan^2\psi|^{1/2}}$ in the Equation 1 tends to infinity. This term can be rewritten as

$$\cos^{-5/2}\psi \frac{(1 + 2\sin^2\psi)^{1/4}}{(\cos^2\psi - 2\sin^2\psi)^{1/2}}. \quad (\text{A.1})$$

Hence, by multiplying the KW pattern by the term $\cos^{5/2}\psi$, the source of singularity regions for the pattern simplifies. We show in Figure A the term $\cos^{5/2}\psi$ in the divergent and in the transverse wave.

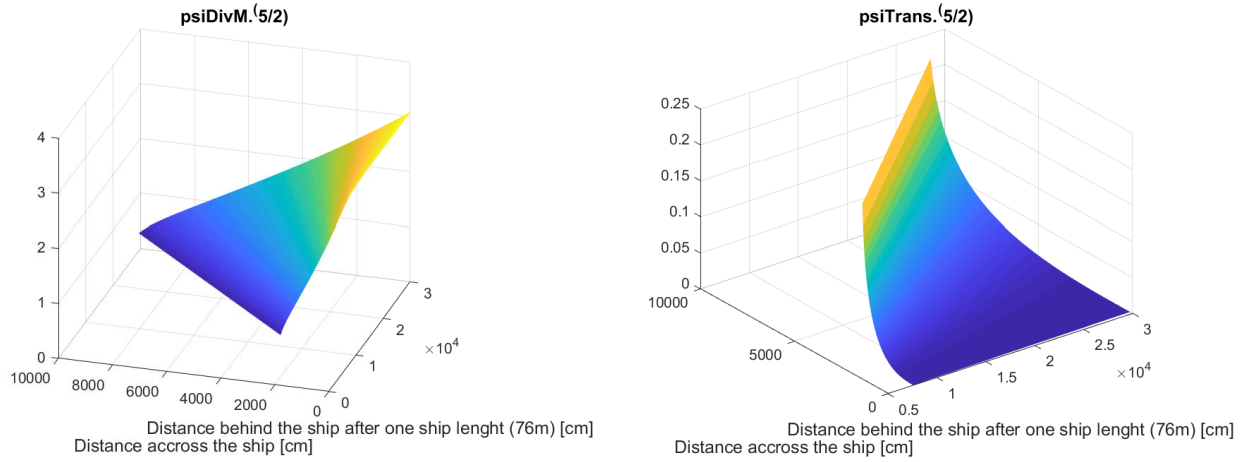


Figure A.1: The term $\cos^{5/2}\psi$ in the divergent wave (left) and in the transverse wave (right).

| DOCUMENT CONTROL DATA | | |
|--------------------------------------------------------------------------------------------------------------------------------------------------------------------------------------------------------------------------------------------------------------------------------------------------------------|------------------------------------------------------------------------------------------------------------------------------------------------|-------------------------------------------------------------|
| *Security markings for the title, authors, abstract and keywords must be entered when the document is sensitive | | |
| 1. ORIGINATOR (Name and address of the organization preparing the document. A DRDC Centre sponsoring a contractor's report, or a tasking agency, is entered in Section 8.) DRDC – Valcartier Research Centre 2459 de la Bravoure Road, Québec QC G3J 1X5, Canada | 2a. SECURITY MARKING (Overall security marking of the document, including supplemental markings if applicable.) CAN UNCLASSIFIED | |
| | 2b. CONTROLLED GOODS NON-CONTROLLED GOODS DMC A | |
| 3. TITLE (The document title and sub-title as indicated on the title page.) The Kelvin Wake Infrared Radiance Model: Implementation into the Sea Surface Infrared Radiance Simulator | | |
| 4. AUTHORS (Last name, followed by initials – ranks, titles, etc. not to be used. Use semi-colon as delimiter) Issa, V.; Daya, Z. A. | | |
| 5. DATE OF PUBLICATION (Month and year of publication of document.) February 2019 | 6a. NO. OF PAGES (Total pages, including Annexes, excluding DCD, covering and verso pages.) 21 | 6b. NO. OF REFS (Total cited in document.) 11 |
| 7. DOCUMENT CATEGORY (e.g., Scientific Report, Contract Report, Scientific Letter) Scientific Report | | |
| 8. SPONSORING CENTRE (The name and address of the department project or laboratory sponsoring the research and development.) DRDC – Valcartier Research Centre 2459 de la Bravoure Road, Québec QC G3J 1X5, Canada | | |
| 9a. PROJECT OR GRANT NO. (If appropriate, the applicable research and development project or grant number under which the document was written. Please specify whether project or grant.) 11gf | 9b. CONTRACT NO. (If appropriate, the applicable contract number under which the document was written.) | |
| 10a. DRDC DOCUMENT NUMBER DRDC-RDDC-2018-R246 | 10b. OTHER DOCUMENT NO(s). (Any other numbers which may be assigned this document either by the originator or by the sponsor.) | |
| 11a. FUTURE DISTRIBUTION WITHIN CANADA (Approval for further dissemination of the document. Security classification must also be considered.) Public release | | |
| 11b. FUTURE DISTRIBUTION OUTSIDE CANADA (Approval for further dissemination of the document. Security classification must also be considered.) Public release | | |

12. KEYWORDS, DESCRIPTORS or IDENTIFIERS (Use semi-colon as a delimiter.)

DRDC Scientific Report; sea surface reflectivity; sea surface emissivity; sea surface roughness; infrared sea radiance; sky radiance; trailing wake; Kelvin wake; turbulent wake

13. ABSTRACT/RÉSUMÉ (When available in the document, the French version of the abstract must be included here.)

The well known 'V' shaped ship Kelvin wake consists of a pattern of sea surface waves with predictable elevation and orientation. In the middle wave infrared, the surface waves are simultaneously emitters and reflectors. The radiance pattern from the Kelvin wake can be exploited for strategic surveillance, smart tracking algorithms and for naval platform vulnerability assessment. We have modeled the middle wave infrared radiance of the Kelvin wake of a ship approximated by a point source of pressure on the surface of infinitely deep water. The elevation field of the Kelvin wake is normalized against measurements from a ship trial. This elevation input is then meshed into facets whose orientation are calculated numerically with a central finite difference scheme. Thereafter we have used the Sea Surface Radiance Simulator, a in-house Matlab code, to calculate the middle wave infrared radiance emitted and reflected by each facet toward an observer. The calculation takes into account the source-receiver geometry, the environmental radiometric sources, and the effects of propagation through the atmosphere. Since there are on the order of a million surface facets, we have clustered facets with the same slopes and relative receiver position. This clustering accelerates significantly the numerical calculation. We find that the mid wave infrared radiance of the Kelvin wake and its contrast with the sea surface background is highly dependent on the receiver position which determines which slopes in the wake are strongly reflecting and emitting in the direction of the receiver. Our Sea Surface Radiance Simulator, with the addition of the Kelvin wake modeling module, now has the capability to calculate the radiance of the three components of ship wakes (Kelvin, turbulent and white water) as well as that of the sea background. Experimental validation of the Kelvin wake midwave infrared radiance against a comprehensive measurement data set is currently being undertaken.

Le « V » caractéristique du sillage de Kelvin créé par le passage d'un bateau consiste en un agencement d'ondes à la surface de la mer possédant une amplitude et une orientation prévisibles. Les ondes de surface sont simultanément émettrices et réfléchissantes dans l'infrarouge moyen. Le modèle de luminance énergétique produit par le sillage de Kelvin peut être exploité à des fins de surveillance stratégique, d'établissement d'algorithmes de poursuite intelligente et d'évaluation de la vulnérabilité de la plateforme navale. Nous avons modélisé la luminance énergétique du sillage de Kelvin d'un navire dans l'infrarouge moyen représentée approximativement par une source ponctuelle de pression à la surface d'eau de mer très profonde. Le champ des données d'amplitude du sillage de Kelvin est normalisé avec des mesures obtenues au cours d'essais réalisés avec un navire. Ces données d'amplitude ont ensuite été intégrées à des facettes dont l'orientation est calculée numériquement selon une méthode des différences finies. Par la suite, nous avons utilisé le programme de luminance énergétique à la surface de la mer, programme interne Matlab, pour calculer la luminance énergétique dans l'infrarouge moyen émise et réfléchi par chaque facette vers un observateur. Le calcul tient compte de la géométrie source récepteur, des sources radiométriques environnementales et des effets de la propagation dans l'atmosphère. Puisqu'il existe environ un million de facettes à la surface, nous les avons regroupées selon leur pente et leur position par rapport au récepteur. Ce regroupement accélère considérablement le calcul numérique. Nous avons découvert que la luminance énergétique dans l'infrarouge moyen du sillage de Kelvin et son contraste par rapport à la surface de la mer environnante dépend grandement de la position du récepteur. Celle-ci détermine quelles pentes du sillage reflètent fortement et émettent dans la direction du récepteur. Le programme de luminance énergétique à la surface de la mer, combiné au module de modélisation du sillage de Kelvin, a maintenant la capacité de calculer la luminance énergétique des trois composantes du sillage des navires (sillage de Kelvin, turbulences et bouillonnements) de même que la mer environnante. La validation expérimentale de la luminance énergétique dans l'infrarouge moyen du sillage de Kelvin par rapport à un ensemble exhaustif de données de mesure est toujours en cours.